Acarel, D., Bulut, F., Bohnhoff, M., Kartal, R. (2014): Coseismic velocity change associated with the 2011 Van earthquake (M7.1): Crustal response to a major event. - *Geophysical Research Letters*, *41*, 13, p. 4519-4526.

DOI: http://doi.org/10.1002/2014GL060624

AGU PUBLICATIONS

Geophysical Research Letters

RESEARCH LETTER
10.1002/2014GL060624

Key Points:
- A coseismic velocity change
- The 2011 Van earthquake
- Scaling between the velocity change and slip

Correspondence to:
D. Acarel,
acarel@gfz-potsdam.de

Citation:
Acarel, D., F. Bulut, M. Bohnhoff, and R. Kartal (2014), Coseismic velocity change associated with the 2011 Van earthquake (*M*7.1): Crustal response to a major event, *Geophys. Res. Lett.*, *41*, 4519–4526, doi:10.1002/2014GL060624.

Received 28 MAY 2014
Accepted 21 JUN 2014
Accepted article online 24 JUN 2014
Published online 10 JUL 2014

Coseismic velocity change associated with the 2011 Van earthquake (*M*7.1): Crustal response to a major event

Diğdem Acarel[1], Fatih Bulut[1], Marco Bohnhoff[1,2], and Recai Kartal[3]

[1]GFZ German Research Centre for Geosciences, Potsdam, Germany, [2]Institute of Geological Sciences, Free University Berlin, Berlin, Germany, [3]Earthquake Department, Turkish Republic Disaster and Emergency Management Presidency, Ankara, Turkey

Abstract Monitoring coseismic velocity changes is a major challenge, since the Earth crust has to be uniformly sampled at preseismic, coseismic, and postseismic stages using repeating active or natural sources. Here we investigate the crustal response to the 2011 Van/Turkey earthquake using ambient noise, which provides the best possible temporal resolution. Combined recordings from the nearest five broadband stations are analyzed for a time period of 6 months framing the main shock. We observe a coseismic velocity decrease of up to 0.76% in the vicinity of the main shock in the frequency range of 0.05–0.3 Hz. The velocity drop is largest at close proximity to the earthquake hypocenter and decreases systematically with distance. We also find a correlation between coseismic velocity decrease and the amount of coseismic slip on the rupture plane. The observed velocity drop shows the drastic response of the brittle crust in response to a major earthquake.

1. Introduction

Large earthquakes represent significant elastic responses of the brittle part of the Earth's crust as the strain energy accumulated typically over hundreds of years is released within a few seconds. This drastic short-term acceleration in deformation rate during a large earthquake diverts the near-fault damage, state of stress, and pore pressure [e.g., *Toksöz et al*., 1976; *Christensen and Wang*, 1985; *Vidale and Li*, 2003]. The compound of such changes is therefore abruptly reflected in the changes of elastic parameters of the surrounding medium such as, e.g., seismic velocity [*Rubinstein and Beroza*, 2004].

Temporal changes of the seismic velocity have been studied for several decades using repeating earthquakes [e.g., *Poupinet et al*., 1984; *Baisch and Bokelman*, 2001] and explosions and aftershocks [e.g., *Li et al*., 1998; *Nishimura et al*., 2000]. The principal study by *Poupinet et al*. [1984] verified a 0.2% velocity drop following the *M*5.9 Coyote Lake Earthquake in 1979 using comparison of coda waves from two repeating earthquakes. Theoretically, the seismic velocity might change even in case of small variations in the spatial distribution of scatterers [*Snieder et al*., 2002; *Snieder*, 2006]. Such a perturbation modifies the observed seismic signals radiated by repeating earthquakes sampling the same source-receiver path at different time spots. However, the occurrence of repeating earthquakes is limited to a few specific regions resulting in a poor spatial coverage on a global scale and thus does not provide a generalized scheme for investigating potential temporal changes due to major earthquakes.

Time-lapse active seismic experiments have been proposed as an alternative approach to investigate temporal changes of the seismic velocity field. *Nishimura et al*. [2000] observed a 0.3–1.0% decrease in velocity using two separate controlled-source experiments before and after the 1998 *M*6.1 Mount Iwate earthquake, respectively. Using repeated seismic profiles to monitor temporal velocity changes in the crust provides a reasonably good spatial resolution due to a controlled source-receiver geometry. However, such experiments involve huge costs and therefore do not represent a feasible tool for a systematic analysis of earthquake-related changes of seismic velocity.

Since ambient noise is continuous in time and space, it provides an alternative tool to monitor potential temporal changes of the crustal seismic velocity. The basic idea is to treat reconstructed Green's functions from cross correlations of continuous ambient seismic noise recordings as a substitute for seismograms generated by, e.g., repeating earthquakes or active sources [*Brenguier et al*., 2011; *Chen et al*., 2010; *Zaccarelli et al*., 2011; *Liu et al*., 2014]. The emergence of the Green's function from the correlation of diffuse wavefields between two sensors has been first demonstrated by ultrasonic and thermal noise laboratory experiments [*Weaver and Lobkis*, 2001; *Lobkis and Weaver*, 2001]. The method later extended to field scale by *Campillo and*

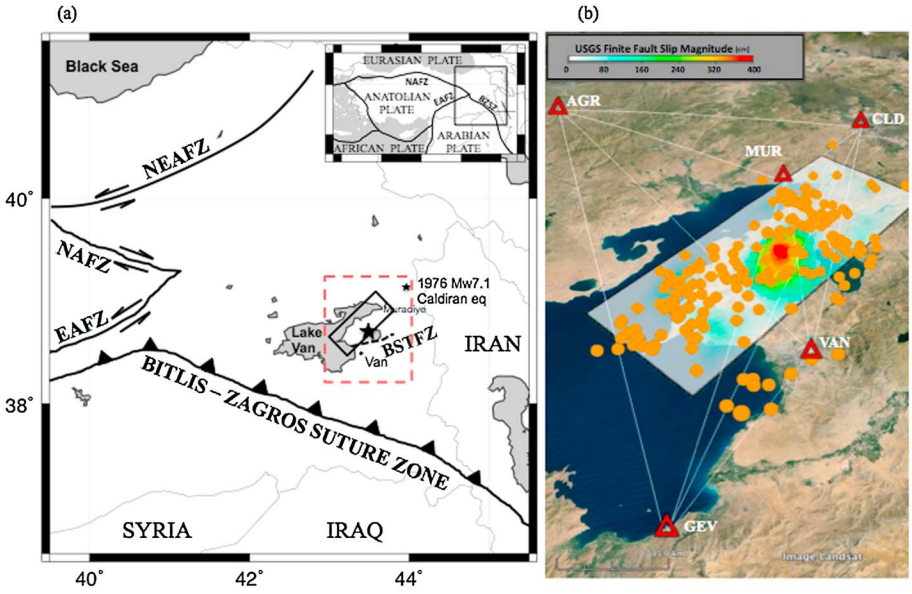

Figure 1. (a) Tectonic setting of the study area: North Anatolian Fault Zone (NAFZ), East Anatolian Fault Zone (EAFZ), North-East Anatolian Fault Zone (NEAFZ), Bitlis-Zagros Suture Zone, and Bardakçı-Saray Thrust Fault Zone (BSTFZ). The large star indicates the hypocenter of the 2011 Van earthquake. (b) Rupture plane (projected white rectangle), coseismic slip distribution (color encoded with warm colors corresponding to high values reaching 4 m) [both after *Hayes*, 2011], and $M > 4$ aftershocks of the 2011 Van *M*7.1 earthquake (yellow circles). Red triangles and white lines are broadband stations and interstation raypaths used in this study, respectively.

Paul [2003] estimating Green's functions from the correlation of seismic coda waves. Moreover, *Shapiro and Campillo* [2004] and *Shapiro et al*. [2005] reconstructed Green's functions by correlating the ambient noise field between two seismometers. In another attempt, the emergence of the scattered waves from the correlations of seismic ambient noise was demonstrated by *Wegler and Sens-Schönfelder* [2007].

In this study, we investigate coseismic velocity perturbations related to the *M*7.1 2011 Van earthquake, eastern Turkey, using ambient noise recorded between July 2011 and January 2012. We analyze velocity perturbations as a function of distance to the earthquake hypocenter and main shock maximum slip along the raypath, respectively, in order to further elaborate on the spatial distribution of elastic response of the Earth's crust to a $M > 7$ earthquake. To capture potential velocity changes, we constructed cross-correlation functions from 6 month long continuous recordings of five local broadband stations framing the time of the main shock.

2. The 2011 Van Earthquake

Eastern Turkey has been struck by a *M*7.1 earthquake, on 23 October 2011 occurring near the city of Van, east of the Karlıova triple junction (Figure 1). The earthquake activated a reverse fault with the hypocenter being located at 16 km depth (http://www.usgs.gov) and with a coseismic slip maximum of 4 m [*Hayes*, 2011]. The rupture plane is striking NE, dipping toward the NW in a NW-SE compressional stress field with a small left-lateral component [*Doğan and Karakas*, 2013].

Eastern Turkey accommodates a highly elevated morphology due to the continental collision between stable Eurasia and the northward migrating Arabian plate [*Sengör and Yılmaz*, 1981]. The three main plate boundaries in eastern Turkey are the right-lateral North Anatolian Fault Zone (NAFZ), the left-lateral East Anatolian Fault Zone (EAFZ), and the Bitlis-Zagros Suture Zone [*Bulut et al*., 2012] (Figure 1a). Interestingly, the 2011 Van earthquake occurred off the main plate boundary on the Bardakçı-Saray Thrust Fault Zone (BSTFZ, Figure 1a). The surface rupture is limited to a length of 8 km, indicating that most of the main shock slip occurred below the surface. Therefore, the fault accommodating the 2011 Van earthquake has been interpreted to be a blind thrust fault to a large extent [*Doğan and Karakas*, 2013]. The aftershocks are distributed mostly outside the nucleation zone extending beneath Lake Van in the west and toward the town of Muradiye in the east, near the epicenter of the *M*7.1 1976 Çaldıran earthquake (Figure 1b). The region falling between the eastern tip

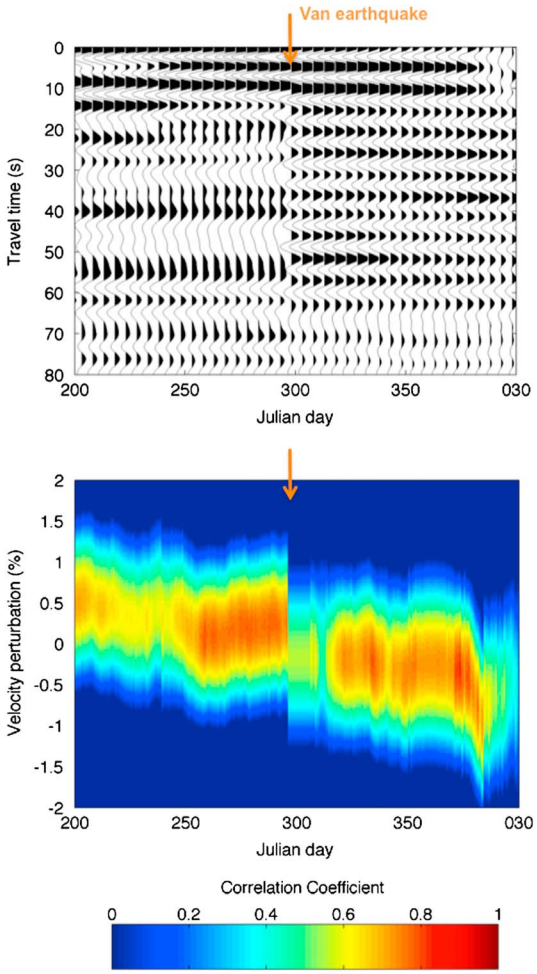

Figure 2. (a) Daily cross correlations for the station pair VAN-CLD, band-pass filtered between 0.05 and 0.3 Hz. The orange arrow indicates the time of the 23 October 2011, Van earthquake. The difference in the correlations before and after the earthquake is evident. (b) The velocity perturbation calculated from the time shifts by comparing each daily cross correlation in Figure 2a with the corresponding reference cross correlation and the correlation coefficient. Following the main shock, an abrupt decrease in seismic velocity can be seen.

of the 2011 Van aftershock activity and the 1976 Çaldıran rupture zone did not host a major earthquake since 1976 and therefore probably represents a highly stressed fault segment [*Akıncı and Antonioli*, 2012].

3. Data Analysis

We use continuous waveform recordings of five broadband stations operated by the Kandilli Observatory and Earthquake Research Institute in Istanbul (KOERI) (stations AGR, CLD, and VAN), and the Turkish Disaster and Emergency Presidency in Ankara (AFAD) (stations GEV and MUR) (Figure 1b) thereby providing 10 interstation raypaths covering different parts of the main shock rupture and the surrounding area. The station CLD lacks 1 month data from 20 days before to 10 days after the Van earthquake. Moreover, stations MUR and VAN lack data on the day of the main shock. Prior to the preprocessing, all waveform recordings were uniformly downsampled to 10 Hz. We follow the data preprocessing steps described in *Bensen et al.* [2007]: First, the mean, trend, and instrument response are removed. In a second step, one-bit normalization is applied to the continuous data to reduce the potential contamination of the waveforms by local seismicity and to minimize the instrumental irregularities. Additionally, we eliminate ~14.000 Van aftershocks with $M > 1.8$ as reported in the AFAD earthquake catalogue from the waveform recordings (http://www.deprem.gov.tr/sarbis/Shared/Default.aspx). This is done since aftershocks are a potential source of uncertainty for our study. Finally, we apply spectral whitening within the bandwidth of the data to balance the frequency spectrum. At this stage, we do not perform band-pass filtering to keep all available information in the waveform recordings. We analyze the time period of July 2011 to January 2012, thus evenly framing the 2011 Van earthquake that occurred in October 2011. A daily cross correlation is computed by stacking nonoverlapping 3 min long time windows moving along a 6 month long data stream. We do not include the main shock day.

The direct surface waves are highly sensitive to the temporal variations of internal sources, such as aftershocks [*Wegler et al.*, 2009]. In a strongly scattering medium, the coda waves repeatedly sample the same region and therefore are more sensitive to small changes within the medium [*Snieder et al.*, 2002; *Snieder*, 2006]. We apply the stretching technique [*Wegler and Sens-Schönfelder*, 2007] focusing on the coda part of the stacked cross-correlation functions to attenuate the effect of internal sources. The coda window to be used for the temporal analysis is selected as a 60 s wide band starting ~10 s after the energy of the direct waves decrease at all five stations. We perform time domain cross correlations on the vertical components, assuming that within the frequency band of interest the coda part of the correlations is composed of surface waves [*Margerin et al.*, 2009; *Froment et al.*, 2013] thus focusing on the Rayleigh-type ambient noise field.

We first calculate a mean cross-correlation function out of all daily correlations to be used as a reference trace. This reference cross correlation is then compared with each individual/daily cross correlation, which is further

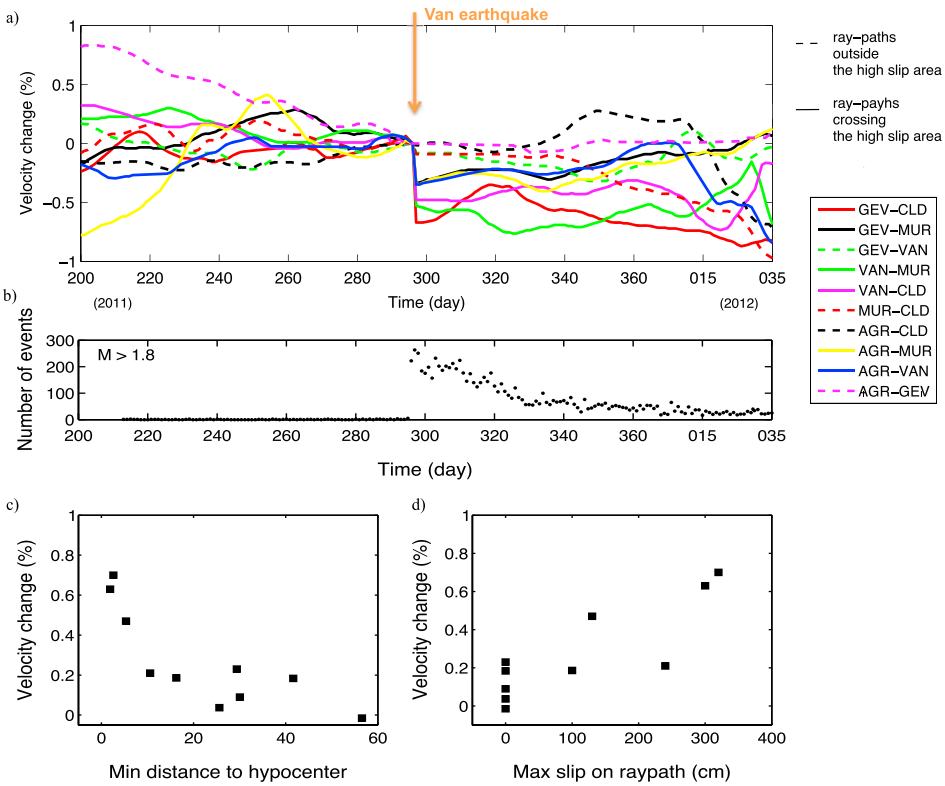

Figure 3. (a) Normalized velocity change with time for all 10 station pairs. Solid and dashed lines indicate station pairs with raypaths crossing and bypassing the main shock rupture zone, respectively. (b) $M > 1.8$ earthquakes in the Van area throughout the time period studied here. All shown events have been discarded from the waveform recordings to exclude any impact on our observations. Observed velocity change plotted (c) with minimum distance of the respective raypath to the Van earthquake hypocenter and (d) with maximum coseismic slip crossed by the ray paths, respectively.

smoothened (moving window average over the following 30 days) in order to calculate corresponding time shifts (Figure 2a).

The method elongates the time axis of the individual correlation with a stretching parameter (by stretching or compressing) and interpolates the amplitude of this trace. The reference trace and the individual traces are then cross correlated to measure the relation between the stretching parameter and the corresponding waveform similarity [*Wegler and Sens-Schönfelder*, 2007; *Minato et al.*, 2012]. A grid search algorithm is performed to find the stretching parameter providing the best possible correlation coefficient (Figure 2b). The resulting stretching parameters allow to estimate the relative time shifts and therefore the corresponding velocity changes during the time period analyzed [*Hadziioannou et al.*, 2009].

All 10 raypaths between the station pairs are included in our analysis in order to investigate potential coseismic velocity perturbations in the near vicinity of the main shock hypocenter with the best possible spatial coverage and resolution. The time shifts observed for coda waves are caused by changes within an area remaining between the stations [*Wegler et al.*, 2009]. Based on the distribution of available interstation distances, we consider the cross correlations within the frequency band of 0.05–0.3 Hz. The frequency band of 0.05–0.3 Hz corresponds to a wide depth range between 5 and 20 km, mixing the effects of middle and upper crust. Therefore, we further analyze the depth extent of the velocity change within three different frequency subbands: 0.05–0.08, 0.08–0.14, and 0.14–0.26 Hz to better interpret the changes in velocity.

4. Results

The most prominent feature observed within the 0.05–0.3 Hz frequency band is an instantaneous velocity decrease corresponding to the main shock origin time of the Van earthquake (Figure 3a). As discussed earlier,

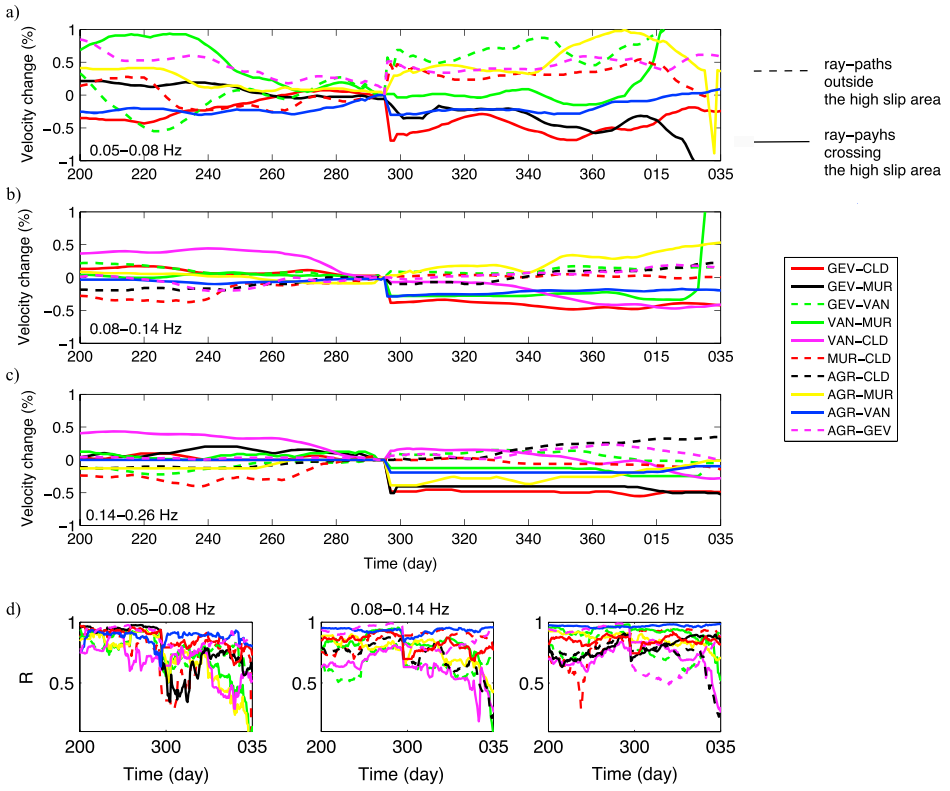

Figure 4. Velocity change observed at three different frequency subbands: (a) 0.05–0.08 Hz (corresponding to upper mid-crustal depths), (b) 0.08–0.14 Hz, and (c) 0.14–0.26 Hz. The drop in velocity within the high-slip area is observed in all subbands. At the longer period band shown in Figure 4a, there is an increase in velocity for the raypaths sampling the area outside the high-slip zone (Figure 1b). (d) Correlation coefficients (*R*) for the daily versus reference cross-correlation functions for each of the three subbands as a measure for the reliability of the velocity change curves in Figures 4a–4c.

we eliminate the ~14.000 Van aftershocks ($M > 1.8$) from the continuous seismic recordings thereby excluding their influence on our results (Figure 3b).

We observe that the velocity drops vary depending on station pairs. In particular, the station pairs GEV-CLD (0.76%), VAN-MUR (0.55%), VAN-CLD (0.54%), GEV-MUR (0.36%), and AGR-VAN (0.35%), all sampling the high-slip area, capture an abrupt coseismic velocity change in the range of 0.3–0.8%. In contrast, station pairs AGR-MUR (0.2%), MUR-CLD (0.1%), and AGR-CLD (0.01%), all with paths outside the high-slip area, do not outline a major velocity change.

To further elaborate on these findings, we plot the obtained coseismic velocity change with minimum distance of the respective raypath to the main shock hypocenter. We find that the drop in seismic velocity decreases with (the minimum) distance to the hypocenter (Figure 3c). Furthermore, we note that the station pairs with highest velocity changes all have raypaths passing consistently through or nearby the main shock nucleation zone while the pairs showing small velocity changes MUR-CLD (0.1%), AGR-CLD (0.01%) have raypaths with relatively larger distances to the main shock hypocenter. Similarly, we compare the observed coseismic velocity changes with corresponding coseismic slip on the rupture plane. We observe that the coseismic velocity drop scales with the maximum coseismic slip within the crustal volume sampled by the respective raypath between the corresponding station pairs (Figure 3d).

The observed velocity changes in the 0.08–0.14 Hz and 0.014–0.26 Hz subbands, corresponding to relatively upper crustal layers, are almost identical (Figures 4b and 4c). Similar to the main frequency band of 0.05–0.3 Hz, we observe a drop in velocity scaling with the minimum distance of the ray path to the hypocenter. The highest velocity drops in the 0.08–0.14 Hz and 0.14–0.26 Hz subbands are on the order of 0.50%, observed for the station pair GEV-CLD, which represents the closest raypath to the nucleation zone. For the time period of our analysis, we observe a steady variation in the preseismic stage and no velocity recovery during the postseismic stage.

Interestingly, in the subband of 0.05–0.08 Hz corresponding to approximately middle crustal depths (12–20 km) [*Vanacore et al*., 2013], there is a clear velocity increase between the station pairs with raypaths outside the high-slip area GEV-VAN (0.50%), MUR-CLD (0.29%), AGR-MUR (0.27%), and AGR-GEV (0.23%). A drop in velocity is still apparent between the station pairs crossing the high-slip area: VAN-CLD (0.54%), GEV-CLD (0.45%), AGR-VAN (0.22%), and GEV-MUR (0.20%). In addition to the velocity change curves, the correlation coefficient (R) between the reference and daily correlation for each frequency subband for all raypaths is shown in Figure 4d as a measure for the reliability of the observations following *Wegler et al*. [2009] and *Hobiger et al.* [2012]. As it is stated in *Wegler et al*. [2009], a low R value may indicate some additional changes to the velocity change such as a variation in the distribution of noise sources. A low R value here refers to values below 0.5–0.6 [*Wegler et al*., 2009; *Bulut et al*., 2011]. In our case the correlation coefficients (R) are usually well above 0.5 on average suggesting that the observed coseismic velocity changes are reliable. The velocity change curves at the long-period subband vary considerably in preseismic and postseismic stages compared to the short-period subbands. Measurements performed by using the coda part of the correlations become more difficult at long periods, due to weaker scattering and slower convergence of noise correlations to empirical Green's functions [*Froment et al*., 2013]. This may be the reason for R values as low as 0.4 observed in this subband. Moreover, the variation in velocity change after day 015 can be explained by the insufficient amount of days stacked.

In general, a velocity recovery is not observed on any raypaths for the short-period subbands. However, at long periods, there is a sharp drop in velocity for the VAN-CLD raypath at the time of the main shock but, in general, no stable trend is observed (Figure 4a). At shorter periods, there is a slight decrease in velocity before the main shock and an immediate recovery back to almost preseismic values in the 0.14–0.26 Hz subband.

5. Discussion

The source area of the M7.1 Van earthquake is characterized by a NW dipping and NE striking rupture plane accommodating a particular patch of high coseismic slip (up to ~ 4 m). This high-slip patch hosts only a few aftershocks and is surrounded by a larger section of reduced coseismic slip that hosts pronounced aftershock activity. The slip is buried to a large extent with a centroid depth of 14 km and constrained to a depth range of 9–20 km [*Elliot et al*., 2013; *Fielding et al*., 2013]. The colocation of the high-slip patch and the patches with dense aftershock activity suggests that the strain accumulated in the near vicinity of the nucleation area has been completely released during the main shock then causing an immediate stress pulse onto neighboring fractures/patches.

Our fundamental observation is that the 2011 M7.1 Van Earthquake results in a velocity drop of up to ~0.8%. This is consistent with the previous studies indicating that major earthquakes may cause a coseismic velocity decrease within the hypocentral region [*Wegler et al*., 2009; *Chen et al*., 2010]. In principle, the amount of stress released during an earthquake (or, in other words, the strain accumulated throughout the interseismic period) might be on the order of $>$10 MPa [e.g., *Oth*, 2013] and is thus significantly larger than the presumable coseismic increase in Coulomb Stress at the tips of the rupture zone ($<$0.5 MPa) [e.g., *King et al*., 1994]. We interpret this to indicate that the elastic response to an earthquake remaining within the Earth is dominated by stress release rather than relatively minor Coulomb Stress increase.

The observed velocity drop in close proximity to the main shock hypocenter points out an impulsive elastic response of the nearby medium to a M7.1 earthquake. The main shock has activated many small-scale faults of different mechanisms within the rupture zone [*Erdik et al*., 2012]. This response might include crack openings, fluid flow, and therefore change in pore pressure deep in the crust. For shallow crustal depths this response might be associated with near-fault damage to the source for a decrease in velocity [*Rubinstein and Beroza*, 2004]. Our observations show a velocity change as a function of distance from the main shock as well as a correlation between the magnitude of the velocity change and the amount of coseismic slip. This suggests that the elastic relaxation is the highest near the hypocenter (coseismic high-slip patch) and decreases with distance from the area most affected by the main shock rupture.

For some station pairs (within the 0.05–0.3 Hz main frequency band), we observe a systematic recovery of the seismic velocity during the first ~80 days following the main shock back to the preseismic levels (Figure 3a, e.g., pairs AGR-MUR, AGR-VAN, and GEV-MUR). There, corresponding raypaths overlap in an area directly west of the high-slip area beneath Lake Van. One might speculate that fresh fracture networks created during the main

shock are being filled with fluids thus balancing the underground pressure and resulting in a temporal recovery of the seismic velocity toward pre–main shock values [*King and Wood*, 1994].

The driving mechanism of the 2011 Van earthquake is thrust faulting dominant at the hypocentral depths, and a small left-lateral component at the shallower parts of the fault plane [*Irmak et al*., 2012]. This is also reflected as an increase in velocity outside the high-slip area and higher magnitude of velocity change in the 0.05–0.08 Hz subband (corresponding to hypocentral depths) compared to the other two relatively shorter period subbands (Figure 4). The increase in the velocity diminishes with depth in correspondence with the reduced thrust component.

6. Conclusions

Ambient noise analysis has been successfully applied to directly measure a coseismic change of seismic velocity in the vicinity of the *M*7.1 2011 Van/eastern Turkey earthquake. The broadband waveform recordings are cross-correlated and stacked for a time period of 6 months framing the main shock.

The observed coseismic velocity decrease in the hypocentral region reaches up to ~0.8% in the frequency band of 0.05–0.3 Hz. The observed velocity drop is largest close to the earthquake hypocenter and decreases with distance from the main shock rupture. A similar correlation is observed between the coseismic velocity decrease and the amount of coseismic slip on the part of the rupture plane penetrated by the corresponding raypaths. Within the frequency band of 0.05–0.08 Hz, corresponding to the Van hypocentral depths, an increase in velocity of about ~0.50% is observed outside the high-slip area, indicating an increase in stress level.

The observation of a drop in crustal velocity in conjunction with a *M*7+ earthquake shows a clear response of the brittle crust pointing out a change in elastic parameters. Such changes can be detected and even monitored with conventional regional seismic networks with interstation spacings of several tens of kilometers and by applying available ambient noise processing techniques.

Acknowledgments

We thank the Turkish Republic Disaster and Emergency Management Presidency (AFAD Earthquake Department) and the Kandilli Observatory and Earthquake Research Institute (KOERI) for providing seismic recordings from selected seismic stations. We thank the German Research Foundation (DFG) for funding within the ICDP priority program (grant Bo 1877/5-1) and the Helmholtz Foundation for funding within the Young Investigators Group: "From microseismicity to large earthquakes." The authors wish to thank the Editor, Michael Wysession, and two anonymous reviewers for their constructive comments that helped to improve the manuscript.

The Editor thanks two anonymous reviewers for their assistance in evaluating this paper.

References

Akıncı, A., and A. Antonioli (2012), Observations and stochastic modelling of strong ground motions for the 2011 October 23 Mw 7.1 Van, Turkey, earthquake, *Geophys. J. Int.*, doi:10.1093/gji/ggs075.

Baisch, S., and G. H. R. Bokelman (2001), Seismic waveform attributes before and after Loma Prieta earthquake: Scattering change near the earthquake and temporal recovery, *J. Geophys. Res.*, *106*(B8), 16,323–16,337, doi:10.1029/2001JB000151.

Bensen, G. D., M. H. Ritzwoller, M. P. Barmin, A. L. Levshin, F. Lin, M. P. Moschetti, N. M. Shapiro, and Y. Yang (2007), Processing seismic ambient noise data to obtain reliable broad-band surface wave dispersion measurements, *Geophys. J. Int.*, *169*, 1239–1260, doi:10.1111/j.1365-246X.2007.03374.x.

Brenguier, F., D. Clarke, Y. Aoki, N. M. Shapiro, M. Campillo, and V. Ferrazzini (2011), Monitoring volcanoes using seismic noise correlations, *Comptes Rendus Geoscience*, *343*(8-9), 633–638.

Bulut, F., W. L. Ellsworth, M. Bohnhoff, M. Aktar, and G. Dresen (2011), Spatiotemporal earthquake clusters along the North Anatolian fault zone offshore Istanbul, *Bull. Seism. Soc. Am.*, *101*(4), 1759–1768, doi:10.1785/0120100215.

Bulut, F., M. Bohnhoff, T. Eken, C. Janssen, and G. Dresen (2012), The East Anatolian Fault Zone: Seismotectonic setting and spatiotemporal characteristics of seismicity based on precise earthquake locations, *J. Geophys. Res.*, *117*, B07304, doi:10.1029/2011JB008966.

Campillo, M., and A. Paul (2003), Long range correlations in the diffuse seismic coda, *Science*, *299*(5606), 547–549, doi:10.1126/science.1078551.

Chen, J. H., B. Froment, Q. Y. Liu, and M. Campillo (2010), Distribution of seismic wave speed changes associated with the 12 May 2008 Mw 7.9 Wenchuan earthquake, *Geophys. Res. Lett.*, *37*, L18302, doi:10.1029/2010GL044582.

Christensen, N., and H. Wang (1985), The influence of pore pressure and confining pressure on dynamic elastic properties of Berea sandstone, *Geophysics*, *50*(2), 207–213, doi:10.1190/1.1441910.

Doğan, B., and A. Karakas (2013), Geometry of co-seismic surface ruptures and tectonic meaning of the 23 October 2011 Mw 7.1 Van earthquake (East Anatolian Region, Turkey), *J. Struc. Geol.*, *46*, 99–114.

Elliot, J. R., A. C. Copley, R. Holley, K. Scharer, and B. Parsons (2013), The 2011 Mw 7.1 Van (Eastern Turkey) earthquake, *J. Geophys. Res. Solid Earth*, *118*, 1619–1637, doi:10.1002/jgrb.50117.

Erdik, M., Y. Kamer, M. Demircoglu, and K. Sesetyan (2012), 23 October 2011 Van (Turkey) earthquake, *Nat. Hazards*, *64*, 651–665.

Fielding, E. J., P. R. Lundgren, T. Taymaz, S. Yolsal-Çevikbilen, and S. E. Owen (2013), Fault-slip source models for the 2011 M7.1 Van earthquake in Turkey from SAR interferometry, pixel offset tracking, GPS and seismic waveform analysis, *Seismol. Res. Lett.*, *84*(4), 579–593, doi:10.1785/0220120164.

Froment, B., M. Campillo, J. H. Chen, and Q. Y. Liu (2013), Deformation at depth associated with the 12 May 2008 Mw 7.9 Wenchuan earthquake from seismic ambient noise monitoring, *Geophys. Res. Lett.*, *40*, 78–82, doi:10.1029/2012GL053995.

Hadziioannou, C., E. Larose, O. Coutant, P. Roux, and M. Campillo (2009), Stability of monitoring weak changes in multiply scattering media with ambient noise correlation: Laboratory experiments, *J. Acoust. Soc. Am.*, *125*(6), 3688–3695.

Hayes, G. (2011), Finite fault model, updated result of the Oct 23, 2011 Mw 7.1 eastern Turkey earthquake. [Available at http://earthquake.usgs.gov/earthquakes/eqinthenews/2011/usb0006bqc/finite_fault.php, last access: May 2014.]

Hobiger, M., U. Wegler, K. Shiomi, and H. Nakahara (2012), Coseismic and postseismic elastic wave velocity variations caused by the 2008 Iwate-Miyagi Nairiku earthquake, Japan, *J. Geophys. Res.*, *117*, B09313, doi:10.1029/2012JB009402.

Irmak, T. S., B. Dogan, and A. Karakas (2012), Source mechanism of the 23 October, 2011, Van (Turkey) earthquake (Mw = 7.1) and aftershocks with its tectonic implications, *Earth Planets Space*, *64*, 991–1003.
King, G. C. P., and R. M. Wood (1994), The impact of earthquakes on fluids in the crust, *Annali di Geofisica*, *37*(6), doi:10.4401/ag-4147.
King, G. C. P., S. S. Ross, and J. Lian (1994), Static stress changes and the triggering of earthquakes, *Bull. Seism. Soc. Am.*, *84*(3), 935–953.
Li, Y.-G., J. E. Vidale, K. Aki, F. Xu, and T. Burdette (1998), Evidence of shallow fault zone strengthening after the 1992 M7.5 Landers, California, earthquake, *Science*, *279*(5348), 217–219, doi:10.1126/science.279.5348.217.
Liu, Z., J. Huang, Z. Peng, and J. Su (2014), Seismic velocity changes in the epicentral region of the 2008 Wenchuan earthquake measured from three-component ambient noise correlation techniques, *Geophys. Res. Lett.*, *41*, 37–42, doi:10.1002/2013GL058682.
Lobkis, O. I., and R. L. Weaver (2001), On the emergence of the Green's function in the correlations of a diffuse field, *J. Acoust. Soc. Am.*, *110*, 3011–3017.
Margerin, L. M., M. Campillo, B. A. Van Tiggelen, and R. Hennino (2009), Energy partition of seismic coda waves in layered media: Theory and application to Pinyon Flats Observatory, *Geophys. J. Int.*, *177*(2), 571–585.
Minato, S., T. Tsuji, S. Ohmi, and T. Matsuoka (2012), Monitoring seismic velocity change caused by the 2011 Tohoku-oki earthquake using ambient noise records, *Geophys. Res. Lett.*, *39*, L09309, doi:10.1029/2012GL051405.
Nishimura, T., N. Uchida, H. Sato, M. Ohtake, S. Tanaka, and H. Hamaguchi (2000), Temporal changes of the crustal structure associated with the M6.1 earthquake on September 3, 1998 and the volcanic activity of mount Iwate, Japan, *Geophys. Res. Lett.*, *27*(2), 269–272, doi:10.1029/1999GL005439.
Oth, A. (2013), On the characteristics of earthquake stress release variations in Japan, *Earth Planet. Sci. Lett.*, *377-378*, 132–141, doi:10.1016/j.epsl.2013.06.037.
Poupinet, G., W. L. Ellsworth, and J. Frechet (1984), Monitoring velocity variations in the crust using earthquake doublets: An application to the Calaveras fault, California, *J. Geophys. Res.*, *89*(B7), 5719–5731, doi:10.1029/JB089iB07p05719.
Rubinstein, J. L., and G. C. Beroza (2004), Evidence for widespread non-linear strong ground motion in the Mw 6.9 Loma Prieta earthquake, *Bull. Seismol. Soc. Am.*, *94*(5), 1595–1608.
Sengör, A. M. C., and Y. Yılmaz (1981), Tethyan evolution of Turkey: A plate tectonic approach, *Tectonophysics*, *75*, 181–241.
Shapiro, N. M., and M. Campillo (2004), Emergence of broadband Rayleigh waves from correlations of ambient seismic noise, *Geophys. Res. Lett.*, *31*, L07614, doi:10.1029/2004GL019491.
Shapiro, N. M., M. Campillo, L. Stehly, and M. H. Ritzwoller (2005), High resolution surface-wave tomography from ambient seismic noise, *Science*, *307*(5715), 1615–1618.
Snieder, R. (2006), The theory of Coda Wave Interferometry, *Pure Appl. Geophys.*, *163*, 455–473.
Snieder, R., A. Gret, H. Douma, and J. Scales (2002), Coda Wave Interferometry for estimating nonlinear behavior in seismic velocity, *Science*, *295*, 2253–2255.
Toksöz, M., C. Cheng, and A. Timur (1976), Velocities od seismic waves in porous rocks, *Geophysics*, *41*(4), 621–645, doi:10.1190/1.1440639.
Vanacore, E. A., T. Taymaz, and E. Saygin (2013), Moho structure of the Anatolian Plate from receiver function analysis, *Geophys. J. Int.*, *193*(1), 329–337, doi:10.1093/gji/ggs1107.
Vidale, J. E., and Y.-G. Li (2003), Damage to the shallow Landers fault from the nearby Hector Mine earthquake, *Nature*, *421*, 524–526.
Weaver, R. L., and O. I. Lobkis (2001), Ultrasonics without a source: Thermal fluctuation correlations at MHz frequencies, *Phys. Rev. Lett.*, *87*, 134301.
Wegler, U., and C. Sens-Schönfelder (2007), Fault zone monitoring with Passive Image Interferometry, *Geophys. J. Int.*, *168*, 1029–1033, doi:10.1111/j.1365-246X.2006.03284.x.
Wegler, U., H. Nakahara, C. Sens-Schönfelder, M. Korn, and K. Shiomi (2009), Sudden drop of seismic velocity after the 2004 M_w 6.6 mid-Niigata earthquake, Japan, observed with Passive Image Interferometry, *J. Geophys. Res.*, *114*, B06305, doi:10.1029/2008JB005869.
Zaccarelli, L., N. M. Shapiro, L. Faenza, G. Soldati, and A. Michelini (2011), Variations of crustal elastic properties during the 2009 L'Aquila earthquake inferred from cross-correlations of ambient seismic noise, *Geophys. Res. Lett.*, *38*, L24304, doi:10.1029/2011GL049750.